

4-22-2011

# Structural Study of Ag-Ge-S Solid Electrolyte Glass System for Resistive Radiation Sensing

Ping Chen

*Boise State University*

Mahesh Ailavajhala

*Boise State University*

Maria I. Mitkova

*Boise State University*

Dmitri A. Tenne

*Boise State University*

Ivan Sanchez Esqueda

*Arizona State University*

*See next page for additional authors*

---

**Authors**

Ping Chen, Mahesh Ailavajhala, Maria I. Mitkova, Dmitri A. Tenne, Ivan Sanchez Esqueda, and Hugh Barnaby

# Structural Study of Ag-Ge-S Solid Electrolyte Glass System for Resistive Radiation Sensing

Ping Chen, Mahesh Ailavajhala  
and Maria Mitkova  
Department of Electrical and  
Computer Engineering,  
Boise State University,  
Boise, ID 83725, U.S.A.

Dmitri Tenne  
Department of Physics,  
Boise State University,  
Boise, ID 83725, U.S.A.

Ivan Sanchez Esqueda and Hugh  
Barnaby  
School of Electrical, Computer, and  
Energy Engineering  
Arizona State University,  
Tempe, AZ 85287, U.S.A.

**Abstract**— Solid electrolytes based on chalcogenide glasses have been one of the most promising candidates for the next generation non-volatile memories. Here we propose a new application of chalcogenide solid electrolytes for low cost, high performance microelectronic radiation sensor that reacts to  $\gamma$ -radiation to produce an easily measurable change in electrical resistance. The active layer material is Ag-doped GeS thin film glasses and several compositions of GeS base glasses were tested for best resistive sensing capability. Energy-dispersive X-ray spectroscopy (EDS) was used for elemental analysis and Raman scattering spectroscopy was measured to determine the structural details and radiation induced structural changes. We also present initial electrical measurement results with test devices.

**Keywords** – radiation induced effects; radiation sensor; solid electrolyte glasses; chalcogenide glasses; resistance change; Raman spectroscopy

## I. INTRODUCTION

Chalcogenide Glasses (ChG) are glasses containing one or more chalcogenide elements of Sulfur (S), Selenium (Se) and Tellurium (Te). Addition of silver to ChG base glasses forms solid electrolytes because Ag has very high mobility in ChG. This has found many applications as sensors, batteries, memory devices [1, 2]. The silver diffusion can be accelerated by radiation and as a result of this, tremendous changes in the electrical properties of the hosting glass can occur. Fig. 1 [3] illustrates the effect of Ag concentration on the electrical conductivity in ChG. Even 0.05 at.% Ag introduced in the chalcogenide matrix causes about one order of magnitude change of the conductivity of ChG. As a result of the intrinsic Radiation Induced Effects (RIE) in the chalcogenide glasses, extensive Ag diffusion and Ag-containing cluster growth can be achieved [4]. This contributes to a stable change in the electrical properties of the resulting material. In this manner the radiation history can be determined. The combination of the two processes (RIE and Ag radiation induced diffusion) has never been used for radiation sensing [5] and we expect to derive significant application benefits from it.

In this work, we report our studies of radiation induced effects in thin films of Ge-S glass and sandwiches of silver and Ge-S chalcogenide glass irradiated with  $\gamma$  rays.

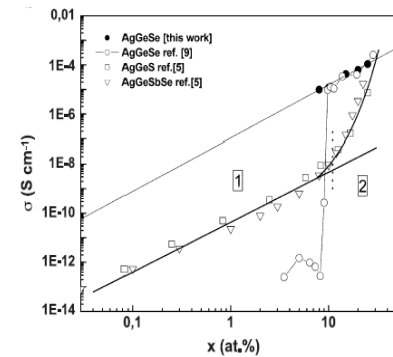


Figure 1. Dependence of the conductivity of several ChG glass systems upon the Ag concentration in them [3].

## II. EXPERIMENTAL

GeS bulk glasses of 4 compositions:  $\text{Ge}_{20}\text{S}_{80}$ ,  $\text{Ge}_{30}\text{S}_{70}$ ,  $\text{Ge}_{33}\text{S}_{67}$  and  $\text{Ge}_{40}\text{S}_{60}$  were alloyed using the conventional melt quench technique. These glasses were then evaporated onto silicon wafers by which amorphous thin films were produced. For material studies, we made 4 types of sample structures – blanket ChG film on Si substrate, blanket ChG film on  $\text{SiO}_2/\text{Si}$  substrate, ChG film covered with Ag film on Si substrate and ChG film covered with Ag film on  $\text{SiO}_2/\text{Si}$  substrate. For electrical measurements, we prepared samples on insulating substrate ( $\text{SiO}_2/\text{Si}$ ) and had both Silver and Tungsten contacts patterned onto the chalcogenide films as shown in Fig. 2.

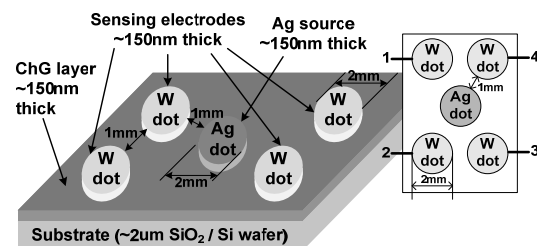


Figure 2. Test device structure patterned with shadow mask.

These material and device samples were then irradiated at Arizona State University (ASU) with  $^{60}\text{Co}$  source. The material

samples were irradiated with different  $\gamma$ -ray doses ranging from 20 krad(Si) to 1.3 Mrad(Si) and were sent to Boise State University (BSU) for materials characterization. All test devices were exposed to 100 krad(Si)  $^{60}\text{Co}$  irradiations and electrically characterized at ASU afterwards. Electrical characterization consisted of DC current-voltage measurements performed with a HP 4146 parameter analyzer.

For samples without Ag, the materials characterization was performed immediately after  $\gamma$  ray irradiation as those radiation-induced structural changes are likely reversible and may diminish overtime. For samples covered with Ag film, excess silver not incorporated in ChG layer was removed by etching with an aqueous solution of Iron III Nitrate ( $\text{Fe}(\text{NO}_3)_3$ ).

To determine the elemental composition and radiation induced Ag incorporation level in the thin film, films were studied using Energy-dispersive X-ray spectroscopy (EDS) by LEO 1430VP Scanning Electron Microscope with EDS accessory.

Raman spectroscopy was measured in a JY-Horiba T64000 machine in triple-subtractive and macro setup. The samples were excited with 441.6 nm blue laser and the power on sample was 60 mW on  $\sim 1\text{mm}$  diameter circle area. The sample chamber was pumped down to ca.  $1 \times 10^{-5}$  Torr to avoid oxidation and the samples were cooled to 100K during Raman measurements. For these thin film samples, we did not see any spot under microscope after extended time of Raman laser irradiation for hours. We did not see any photo darkening effects and the lineshapes remained same over time. Thus we are confident to say the Raman condition of current power density of  $\sim 60 \text{ mW/mm}^2$  and 100 K cooling is safe to generate reproducible results without other light induced effects.

### III. RESULTS AND DISCUSSION

#### A. Film homogeneity by Energy-dispersive X-ray spectroscopy (EDS)

We have produced numerous amounts of samples on different substrates since it is important for us to ensure the sample homogeneity across substrate. EDS was measured on samples evaporated in different batches (batch #1 and #2) and on different substrates (Si and oxidized Si wafer) across the wafer. The results are summarized in Table 1. The results show that the film is quite homogenous since EDS results from different areas and pieces are within 1% of error bar. The sample series evaporated in different batches show variation within 2%. The samples with Ag show same ratio of Ge and S. This is easy to understand since there will be no transmutation and the Ge and S quantity would remain unaffected by Ag diffusion.

TABLE I. EDS RESULTS ON GES AND AG/GES SAMPLES

Non-Ag samples	$\text{Ge}_x\text{S}_{1-x}$	Ag-containing samples	$\text{Ag}_y(\text{Ge}_x\text{S}_{1-x})_{1-y}$
	Ge (x)		Ge (x)
$\text{Ge}_{20}\text{S}_{80}$ , #2	$32.8 \pm 0.1\%$	$\text{Ag}/\text{Ge}_{20}\text{S}_{80}$ , #2	$33.4 \pm 0.1\%$
$\text{Ge}_{30}\text{S}_{70}$ , #1	$34.7 \pm 0.4\%$	$\text{Ag}/\text{Ge}_{30}\text{S}_{70}$ , #1	$35.1 \pm 0.3\%$

$\text{Ge}_{30}\text{S}_{70}$ , #2	$34.6 \pm 0.2\%$	$\text{Ag}/\text{Ge}_{30}\text{S}_{70}$ , #2	$35.2 \pm 0.0\%$
$\text{Ge}_{33}\text{S}_{67}$ , #1	$41.0 \pm 1.0\%$	$\text{Ag}/\text{Ge}_{33}\text{S}_{67}$ , #1	$43.0 \pm 0.4\%$
$\text{Ge}_{40}\text{S}_{60}$ , #2	$44.7 \pm 0.1\%$	$\text{Ag}/\text{Ge}_{40}\text{S}_{60}$ , #2	$44.5 \pm 0.1\%$
$\text{Ge}_{40}\text{S}_{60}$ , #1	$46.2 \pm 0.4\%$	$\text{Ag}/\text{Ge}_{40}\text{S}_{60}$ , #1	$47.7 \pm 0.5\%$

#### B. Structural units in GeS chalcogenide glasses and radiation induced structural changes

Raman is a powerful tool in determining the structure units and quantification of the relative changes of different units. The Ge-S structural common building blocks and corresponding Raman modes / cross sections are well studied in literature [6, 7] and are summarized in Fig. 3. In our studied composition range of Ge percent from 20% to 40%, we can see a systematic increase of ethane-like mode (ETH) around  $250 \text{ cm}^{-1}$  and edge-sharing tetrahedral mode (ES) around  $430 \text{ cm}^{-1}$  in the expense of the decrease of corner sharing tetrahedral mode (CS) around  $340 \text{ cm}^{-1}$ . For the very Ge-rich composition, we can see the appearance of mode from *c*-GeS like distorted rock salt double-layer structure (RL).

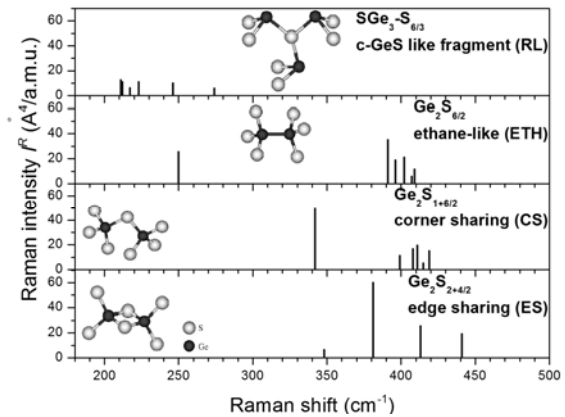


Figure 3. Raman modes and cross sections of different structural units. Adapted from Ref. [7].

Here we show one set of Raman spectra for  $\text{Ge}_{30}\text{S}_{70}$  as in Fig. 4. The observed Raman lineshapes in the  $200 \text{ cm}^{-1}$  to  $500 \text{ cm}^{-1}$  range were fitted using a least squares routine to a superposition of above-mentioned Raman peaks. Detailed quantification results from Raman peak analysis indicated that the structural changes in non-Ag containing samples are mostly reversible as we did not observe any change in lineshapes. While for Ag containing samples, we could see the increase of ETH units, indicating Ge-Ge homopolar bonds. This is because that when the Ag atoms were added to the ChG, they tended to break sulfur bridges and form Ag cation and terminated S anion pairs. The glass network backbone became more Ge-rich and the Ge-Ge homopolar bonds and ETH units would increase.

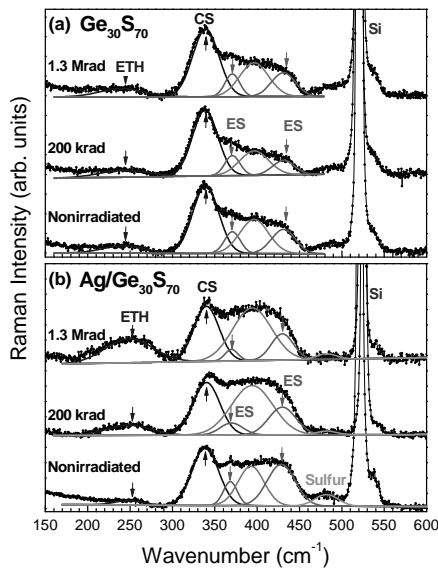


Figure 4. Fitted Raman spectra of (a)  $\text{Ge}_{30}\text{S}_{70}$  and (b)  $\text{Ag}/\text{Ge}_{30}\text{S}_{70}$  samples after irradiation of different  $\gamma$ -ray doses (non-irradiated, 200 krad and 1.3 Mrad). Fitted Gaussian peaks are labeled with corresponding structural units (ETH, CS and ES). Si peak around  $520\text{ cm}^{-1}$  and sulfur chain mode around  $476\text{ cm}^{-1}$  are also labeled.

### C. Ag incorporation level determined from Raman and EDS

The Ag incorporation rates measured from EDS at BSU are plotted in Fig. 5. We can see that there is higher Ag% incorporated with higher  $\gamma$  ray dose.

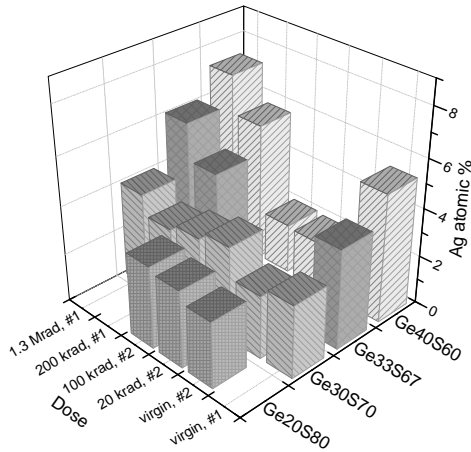


Figure 5. Ag atomic% determined from EDS

It is worth to mention here that we can also verify the Ag% from Raman measurements. In Fig. 6, we show normalized Raman spectra of  $\text{Ge}_{20}\text{S}_{80}$  and  $\text{Ag}/\text{Ge}_{20}\text{S}_{80}$  and their difference spectrum. In all the modes discussed in last section, the S atoms are either 2-fold or 3-fold coordinated and are bridging 2 or 3 atoms. Those modes are all categorized as bridging Ge-S modes. While in the difference spectrum of Fig. 6, the highlighted region is related to terminal Ge-S vibration. These modes are assigned to vibration modes of different types of terminated S anion structure, including dithiogermanate for  $\text{GeS}_{2.5}^-$ , metathiogermanate for  $\text{GeS}_{3.2}^-$  and pyrothiogermanate

for  $\text{GeS}_{3.5}^{3-}$  respectively [8-10]. The total area ratio of those terminal Ge-S modes increases with Ag% monotonically and correlates well with EDS results.

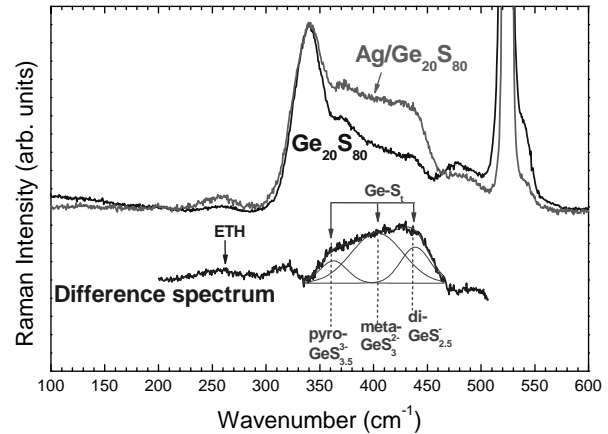


Figure 6. Normalized Raman spectra of  $\text{Ge}_{20}\text{S}_{80}$  and  $\text{Ag}/\text{Ge}_{20}\text{S}_{80}$  and their difference spectrum highlighting terminal Ge-S vibrations.

### D. Initial electrical measurements

In Fig. 7, we show the initial electrical measurements on the lateral test devices. As the figure illustrates, measurements on the device are performed by sweeping DC voltage ( $V_D$ ) across the sensing tungsten (W) electrodes. The current between the electrodes ( $I_D$ ) is sampled at each voltage in the sweep (via a source-monitor unit – SMU), thereby allowing for the resistance between the contacts to be assessed. From the plot we can see resistance decrease after  $\gamma$  ray irradiation of 100 krad(Si).

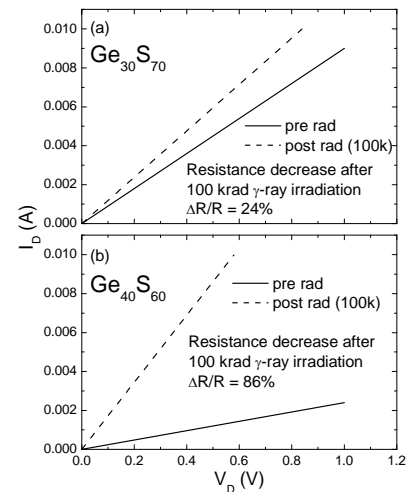


Figure 7. I-V responses of (a)  $\text{Ge}_{30}\text{S}_{70}$  and (b)  $\text{Ge}_{40}\text{S}_{60}$  test devices

## IV. CONCLUSION

The structure of Ge-S and Ag-Ge-S thin films was studied by Raman scattering. We found the Ag incorporation to the base Ge-S glasses with  $\gamma$  ray irradiation verified by both EDS and Raman. The radiation induced structural changes would help silver diffuse and show measurable resistance decrease.

Such device can be very promising future radiation sensing candidate.

#### ACKNOWLEDGMENT

The authors are thankful to Steven Livers for alloying the bulk glasses. We also would like to thank Prof. M. N. Kozicki and his group for help in evaporating the first batch of thin films. This work was supported by a grant from Battelle Energy Alliance under Blanket Master Contract No. 41394.

#### REFERENCES

- [1] M. N. Kozicki, M. Park, and M. Mitkova, "Nanoscale memory elements based on solid-state electrolytes," *IEEE Trans. Nanotechnol.*, vol. 4, pp. 331-338 (2005).
- [2] M. Mitkova, Y. Sakaguchi, D. Tenne, S. K. Bhagat, and T. L. Alford, "Structural details of Ge-rich and silver-doped chalcogenide glasses for nanoionic nonvolatile memory," *physica status solidi (a)*, vol. 207, pp. 621-626 (2010).
- [3] M. Ribes, E. Bychkov, and A. Pradel, "Ion transport in chalcogenide glasses: Dynamics and structural studies," *J. Optoelectron. Adv. Mater.*, vol. 3, pp. 665-674 (2001).
- [4] M. Mitkova, M. N. Kozicki, H. C. Kim, and T. L. Alford, "Local structure resulting from photo and thermal diffusion of Ag in Ge-Se thin films," *J. Non-Cryst. Solids*, vol. 338-340, pp. 552-556 (2004).
- [5] H. Smith and M. Lucas, "Gamma-Ray Detectors," in *Passive nondestructive assay of nuclear materials*, D. Reilly, N. Ensslin, H. Smith, and S. Kreiner, Eds., Los Alamos: Los Alamos National Laboratory, 1991, pp. 43-64.
- [6] K. Jackson, A. Briley, S. Grossman, D. V. Porezag, and M. R. Pederson, "Raman-active modes of  $\alpha$ -GeSe<sub>2</sub> and  $\alpha$ -GeS<sub>2</sub>: A first-principles study," *Phys. Rev. B*, vol. 60, pp. R14985-R14989 (1999).
- [7] R. Holomb, P. Johansson, V. Mitsa, and I. Rosola, "Local structure of technologically modified g-GeS<sub>2</sub>: resonant Raman and absorption edge spectroscopy combined with *ab initio* calculations," *Phil. Mag.*, vol. 85, pp. 2947-2960 (2005).
- [8] B. Barrau, M. Ribes, M. Maurin, A. Kone, and J.-L. Souquet, "Glass formation, structure and ionic conduction in the Na<sub>2</sub>S---GeS<sub>2</sub> system," *J. Non-Cryst. Solids*, vol. 37, pp. 1-14 (1980).
- [9] E. Robinel, B. Carette, and M. Ribes, "Silver sulfide based glasses (I). Glass forming regions, structure and ionic conduction of glasses in GeS<sub>2</sub>---Ag<sub>2</sub>S and GeS<sub>2</sub>---Ag<sub>2</sub>S---AgI systems," *J. Non-Cryst. Solids*, vol. 57, pp. 49-58 (1983).
- [10] E. I. Kamitsos, J. A. Kapoutsis, G. D. Chryssikos, G. Taillades, A. Pradel, and M. Ribes, "Structure and Optical Conductivity of Silver Thiogermanate Glasses," *J. Solid State Chem.*, vol. 112, pp. 255-261 (1994).